JBC RESEARCH ARTICLE

Reciprocal regulatory balance within the CLEC16A–RNF41 mitophagy complex depends on an intrinsically disordered protein region

Received for publication, January 12, 2023 Published, Papers in Press, February 22, 2023,
https://doi.org/10.1016/j.jbc.2023.103057

Morgan A. Gingerich[1,2], Jie Zhu[1], Biaoxin Chai[1], Michael P. Vincent[3,4], Nuli Xie[5], Vaibhav Sidarala[1], Nicholas A. Kotov[5], Debashish Sahu[6], Daniel J. Klionsky[7], Santiago Schnell[3,4], and Scott A. Soleimanpour[1,2,3,8,*]

From the [1]Department of Internal Medicine and Division of Metabolism, Endocrinology & Diabetes, [2]Program in Cellular and Molecular Biology, [3]Department of Molecular and Integrative Physiology, [4]Department of Computational Medicine and Bioinformatics, and [5]Department of Chemical Engineering, University of Michigan, Ann Arbor, Michigan, USA; [6]University of Michigan BioNMR Core Facility, Ann Arbor, Michigan, USA; [7]Life Sciences Institute and Department of Molecular, Cellular, and Developmental Biology, University of Michigan, Ann Arbor, Michigan, USA; [8]Endocrinology and Metabolism Section, Medicine Service, VA Ann Arbor Health Care System, Ann Arbor, Michigan, USA

Reviewed by members of the JBC Editorial Board. Edited by Wolfgang Peti

CLEC16A is an E3 ubiquitin ligase that regulates mitochondrial quality control through mitophagy and is associated with over 20 human diseases. CLEC16A forms a complex with another E3 ligase, RNF41, and a ubiquitin-specific peptidase, USP8; however, regions that regulate CLEC16A activity or the assembly of the tripartite mitophagy regulatory complex are unknown. Here, we report that CLEC16A contains an internal intrinsically disordered protein region (IDPR) that is crucial for CLEC16A function and turnover. IDPRs lack a fixed secondary structure and possess emerging yet still equivocal roles in protein stability, interactions, and enzymatic activity. We find that the internal IDPR of CLEC16A is crucial for its degradation. CLEC16A turnover was promoted by RNF41, which binds and acts upon the internal IDPR to destabilize CLEC16A. Loss of this internal IDPR also destabilized the ubiquitin-dependent tripartite CLEC16A–RNF41–USP8 complex. Finally, the presence of an internal IDPR within CLEC16A was confirmed using NMR and CD spectroscopy. Together, our studies reveal that an IDPR is essential to control the reciprocal regulatory balance between CLEC16A and RNF41, which could be targeted to improve mitochondrial health in disease.

The *CLEC16A* (C-type lectin domain containing 16A) gene is associated with over 20 human diseases including diabetes, cardiovascular disease, stroke, multiple sclerosis, arthritis, and Crohn disease, as well as other inflammatory diseases (1–7). Despite its original designation as a C-type lectin, this is a misnomer as the CLEC16A protein does not actually contain a C-type lectin domain. *CLEC16A* encodes an E3 ubiquitin ligase that maintains mitochondrial health through selective mitochondrial autophagy (mitophagy), which eliminates damaged mitochondria (2, 8). CLEC16A regulates mitophagy by forming a tripartite complex with fellow E3 ubiquitin ligase RNF41/Nrdp1 and the deubiquitinase USP8, which together control activity of the mitophagy regulator PRKN/Parkin (8, 9). Importantly, CLEC16A directly binds and ubiquitinates RNF41 (independent of RNF41 ubiquitin ligase activity) to promote assembly and stability of the tripartite mitophagy complex (8, 10). Loss of CLEC16A impairs mitochondrial health and function in many cell types including pancreatic β-cells, sensory neurons, and immune cells (2, 8, 11–14). Despite strong implications of CLEC16A having a role in disease and in critical cellular processes, its functional domains were left uninvestigated until very recently (14). In particular, CLEC16A domains that control its ubiquitin ligase activity, or regulate assembly of the tripartite mitophagy complex (CLEC16A-RNF41-USP8), remain unknown.

CLEC16A is predicted to contain two intrinsically disordered protein regions (IDPRs): a C-terminal IDPR that stabilizes CLEC16A by inhibiting self-ubiquitination (14) and an unexplored internal putative IDPR. IDPRs lack a fixed secondary structure and their disruption and dysregulation is linked to many human diseases (15–19). IDPRs within E3 ubiquitin ligases are capable of controlling their enzymatic ubiquitin ligase activity and mediating their interactions with partner proteins, among other functions (20, 21). We hypothesized that the putative internal IDPR may play similar roles within CLEC16A by contributing to its ubiquitin ligase activity or mitophagy complex assembly.

Here, we investigate the CLEC16A internal IDPR for key roles in regulating its ubiquitin ligase activity, important protein interactions, and turnover. We observed that disruption of the putative internal CLEC16A IDPR prevented CLEC16A turnover. While the internal CLEC16A IDPR was not a site for auto-ubiquitination, we observed that RNF41 promoted the ubiquitination and destabilization of CLEC16A, and this was dependent on the CLEC16A internal IDPR. Reciprocally, the CLEC16A internal IDPR was required for CLEC16A to bind and ubiquitinate RNF41 and form the tripartite CLEC16A–RNF41–USP8 mitophagy complex. Finally, we confirmed that CLEC16A contains an internal IDPR by several biochemical

* For correspondence: Scott A. Soleimanpour, ssol@med.umich.edu.

and biophysical approaches. Together, we not only clarify crucial structural and functional roles for the CLEC16A internal IDPR but also establish RNF41 as a novel post-translational regulator of CLEC16A stability.

Results

CLEC16A contains a putative internal IDPR

To understand how the internal putative IDPR regulates CLEC16A structure and function, we first investigated CLEC16A *in* silico using multiple computational techniques. Using the highly accurate protein structure prediction tool, AlphaFold, we observed that CLEC16A has a large internal region predicted to lack secondary structure (Fig. 1*A*) (22, 23). Concordantly, the disorder prediction algorithm IUPred2 predicts an internal IDPR that is conserved in human and mouse CLEC16A (Fig. 1*B*) (14, 24). To complement this approach, we investigated the amino acid composition of the putative internal CLEC16A IDPR (amino acids 347–472) compared to the amino acid composition in the validated IDPR dataset Disprot (25). Validated IDPRs are enriched in charged, polar, hydrophilic residues relative to the expected amino acid distribution in nature (14, 26). Indeed, the putative internal CLEC16A IDPR shows significant enrichment for the charged, polar residues glutamic acid (E) and lysine (K) that are known to promote intrinsic disorder (Fig. 1, *C* and *D*) (27). Collectively, these biophysical predictions suggest CLEC16A contains an internal IDPR that spans residues 347 to 472.

Lysine residues within the CLEC16A IDPR are required for CLEC16A turnover

To understand the function of the putative internal IDPR, we introduced focused mutations within this region and investigated their impact on CLEC16A (Fig. 2*A*). IDPRs commonly promote protein degradation, in part due to accessibility for degradative posttranslational modifications (28–30). Thus, we first considered whether the putative internal CLEC16A IDPR affects CLEC16A stability. First, we overexpressed Flag-epitope–tagged WT and mutant forms of CLEC16A in HEK293T cells and evaluated their relative levels *via* Western blot (Fig. 2*B*). We found that a CLEC16A mutant lacking the putative internal IDPR amino acids 347 to 472 (CLEC16A ΔIDPR) was detectable at higher levels than full-length WT CLEC16A (Fig. 2*B*). Next, we assessed protein stability by blocking protein synthesis with cycloheximide. Interestingly, the CLEC16A mutant lacking the internal IDPR maintained higher protein levels and was more stable than WT CLEC16A, indicating that the internal IDPR destabilized CLEC16A (Fig. 2*C*).

We then questioned what features of the CLEC16A internal IDPR might mediate CLEC16A turnover. While CLEC16A is

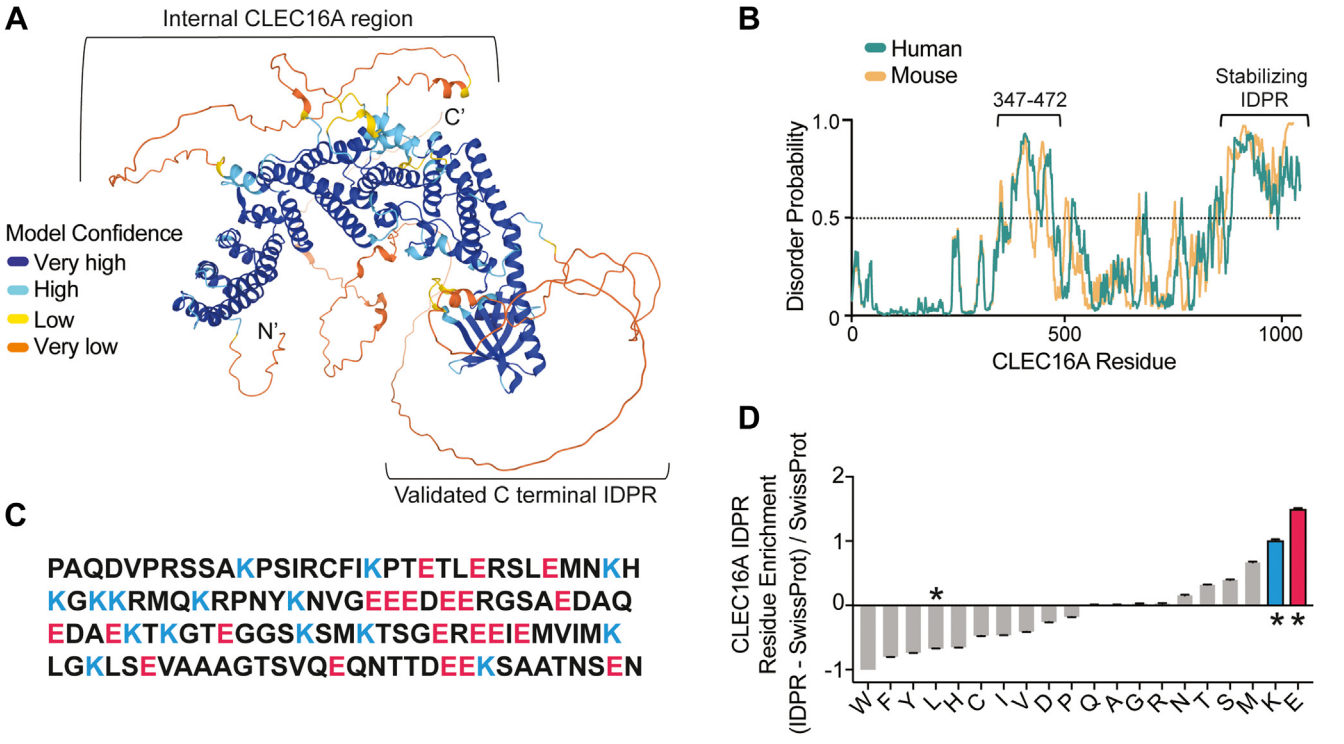

Figure 1. CLEC16A is predicted to contain an internal intrinsically disordered protein region by complementary *in silico* analyses. *A*, structural prediction of CLEC16A using AlphaFold. Model confidence is indicated by the per-residue predicted local distance difference test (pLDDT) from 0 to 100. Very high: pLDDT > 90, High: 90 > pLDDT > 70, Low: 70 > pLDDT > 50, Very low: pLDDT < 50. A low pLDDT score is a competitive predictor of protein disorder (22, 23). *B*, disorder probability of human and mouse CLEC16A from IUPred2. Putative IDPRs were defined with a probability threshold of >0.5. *C*, residues of the mouse CLEC16A putative internal IDPR (AA 347–472), with significantly enriched residues identified in panel (*D*) highlighted (lysine, K, *blue*; glutamic acid, E, *red*). *D*, residue composition bias of the mouse CLEC16A internal IDPR (AA 347–472) generated with Composition. Profiler, comparing residue enrichment of the CLEC16A internal IDPR *versus* SWISS-PROT 51 database. Significantly enriched lysine (*blue*) and glutamic acid (*red*) residues are highlighted. *$p < 0.05$. IDPR, intrinsically disordered protein region.

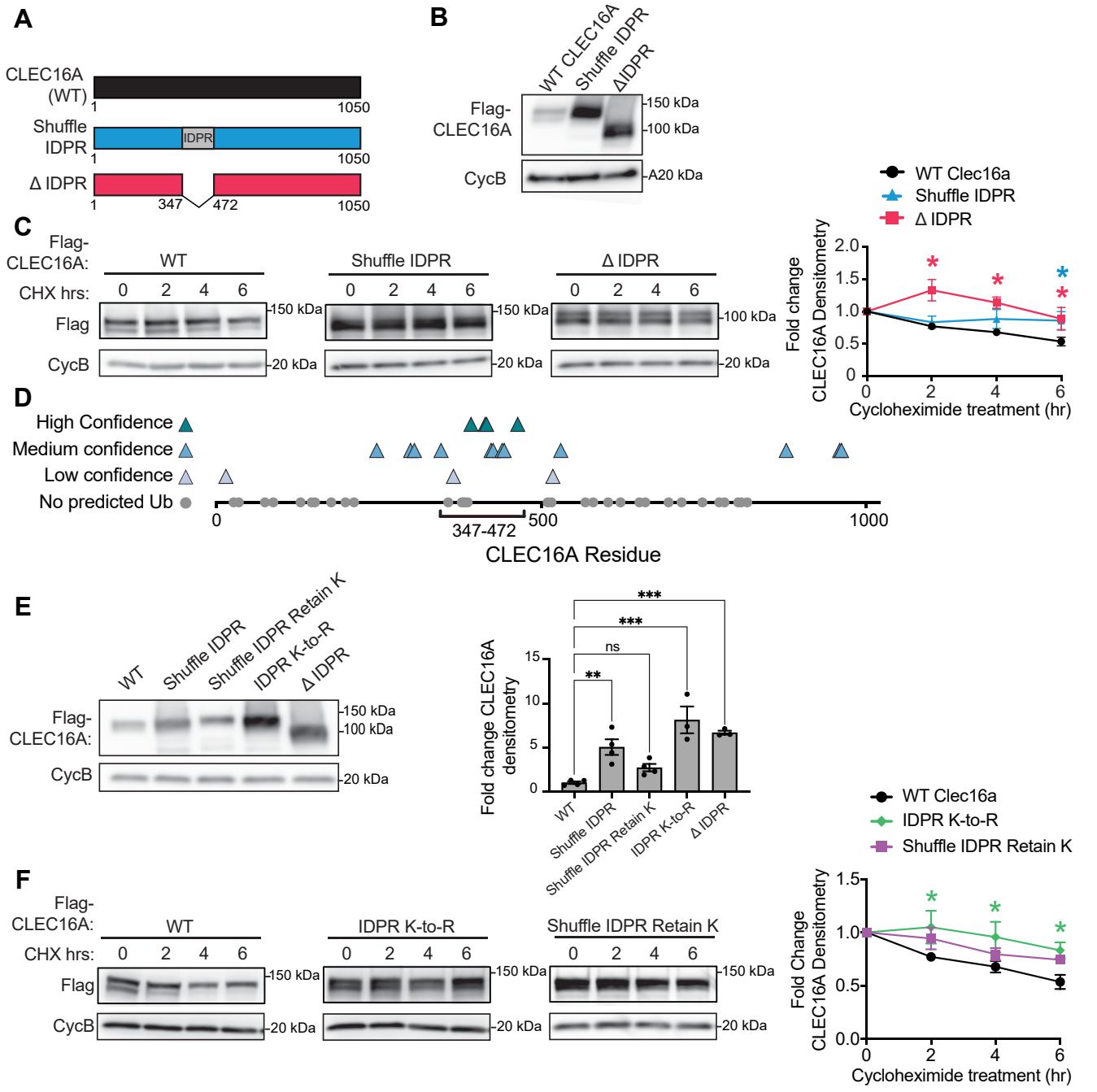

Figure 2. The internal IDPR contains lysine residues that are essential for CLEC16A turnover. *A*, schematic of C-terminal Flag epitope-tagged constructs encoding WT full-length CLEC16A, CLEC16A with the internal IDPR residues randomly shuffled (Shuffle IDPR), or CLEC16A lacking the internal IDPR (ΔIDPR). *B*, representative anti-Flag Western blot (WB) of WT, shuffle IDPR, and ΔIDPR CLEC16A after transfection in HEK293T cells (n = 3/group). *C*, representative WB of Flag-CLEC16A levels from 293T cells transfected with WT, Shuffle IDPR, or ΔIDPR CLEC16A following treatment with 300 μg/ml cycloheximide for 0 to 6 h. Densitometry represents percent change (%) from basal levels normalized to Cyclophilin B (Cyc B) loading control (n = 4/group). *D*, predicted ubiquitination of CLEC16A residues, generated by UbPred. *E*, representative Flag WB of WT, Shuffle IDPR, Shuffle IDPR retain K, IDPR K-to-R, and ΔIDPR CLEC16A following transfection in 293T cells. Densitometry represents fold change in protein levels relative to WT CLEC16A, normalized to Cyc B. No significant differences were found between CLEC16A Shuffle IDPR, IDPR K-to-R, and ΔIDPR (n = 3–4/group). *F*, representative WB of Flag-CLEC16A levels from 293T cells transfected with WT, IDPR1 K-to-R, and Shuffle IDPR retain K CLEC16A following treatment with 300 μg/ml cycloheximide for 0 to 6 h. Densitometry represents % change from basal levels normalized to Cyc B. n = 3/group. *$p < 0.05$; **$p < 0.01$; ***$p < 0.001$. IDPR, intrinsically disordered protein region.

highly conserved in mammals, the internal IDPR overlaps with a region of lower relative conservation (Fig. S1, *A* and *B*). IDPRs functions can be dictated by the order of amino acids, as well as the composition (31, 32). Thus, we tested whether the order of amino acids in the CLEC16A internal IDPR was required to control CLEC16A degradation. To this end, we generated a CLEC16A construct with randomly shuffled residues in the internal IDPR (Shuffle IDPR; Fig. 2*A*). Effectively, this shuffled CLEC16A construct preserves the amino acid composition within the IDPR but not the order of the residues.

We confirmed that shuffling did not introduce known functional domains using SMART and PROSITE domain prediction analyses (data not shown) (33, 34). When compared to WT CLEC16A, shuffling the CLEC16A internal IDPR increased protein levels and stability, similar to the IDPR deletion (Fig. 2, *B* and *C*). These results indicate that the internal IDPR functions in a sequence-dependent manner to destabilize CLEC16A (Fig. 2, *B* and *C*).

We next considered what aspects of the internal CLEC16A IDPR amino acid sequence might mediate CLEC16A degradation. IDPRs are common sites for degradative post-translational modification (28). Moreover, the stability of E3 ubiquitin ligases is often controlled *via* degradative ubiquitination (35). We questioned whether the CLEC16A internal IDPR was a site for ubiquitination that would destabilize CLEC16A. We searched for putative ubiquitination sites on CLEC16A using UbPred, which predicts protein ubiquitination sites based on surrounding amino acid sequence homology to known ubiquitination sites in the proteome (36). We found that the CLEC16A internal IDPR contains an enrichment of lysine residues that are predicted to be ubiquitinated with high confidence (Fig. 2*D*). We therefore generated a CLEC16A mutant construct insensitive to ubiquitination with lysine-to-arginine mutagenesis of the internal IDPR (IDPR K-to-R), which is a substitution strategy that retains a similar residue structure and charge. The CLEC16A IDPR K-to-R mutant had increased protein levels and was significantly more stable than WT CLEC16A and achieved similar levels and stability to CLEC16A mutants bearing a shuffled or truncated internal IDPR (Fig. 2, *E* and *F*). These findings indicate that lysine residues within the internal IDPR are crucial for CLEC16A turnover.

Specific lysine residues can serve as important motifs or degrons that support both the recognition of proteins by an E3 ligase and the subsequent protein degradation (37, 38). Given the importance of lysine residues in the internal IDPR for CLEC16A turnover, we questioned whether the CLEC16A construct with the shuffled IDPR had impaired turnover simply due to the disrupted position and pattern of lysine residues. Thus, we investigated the importance of lysine residue positioning. Specifically, we asked whether lysine positioning within the IDPR was sufficient to mediate CLEC16A turnover, independent of the order of surrounding amino acids. We tested this by retaining the CLEC16A IDPR lysine residues at their original positions while shuffling the remainder of the IDPR, using the same shuffled IDPR sequence as before (Shuffle IDPR Retain K). The Shuffle IDPR retain K CLEC16A construct had a modest increase in levels and stability compared to WT CLEC16A, though this increase was not statistically significant (Fig. 2, *E* and *F*). Thus, the presence and position of lysine residues is the dominant feature to regulate CLEC16A stability, yet the remaining IDPR sequence order may modestly contribute to CLEC16A turnover as well.

CLEC16A does not self-ubiquitinate lysine residues within the internal IDPR in vitro

After identifying the putative internal IDPR as a region that controls CLEC16A turnover, we sought to understand the mechanism by which the lysine residues within the IDPR promote CLEC16A destabilization. Notably, ubiquitin ligases commonly self-ubiquitinate their lysine residues to control their own stability and degradation (35). To determine whether CLEC16A self-ubiquitinates its internal IDPR, we generated recombinant CLEC16A protein and assessed ubiquitination *in vitro*. Upon deleting the CLEC16A IDPR, or shuffling its residues, we observed reduced self-ubiquitination when compared to WT CLEC16A (Fig. 3, *A* and *B*). Unexpectedly, the ubiquitination-resistant CLEC16A IDPR mutant (IDPR K-to-R) showed no impairments in self-ubiquitination

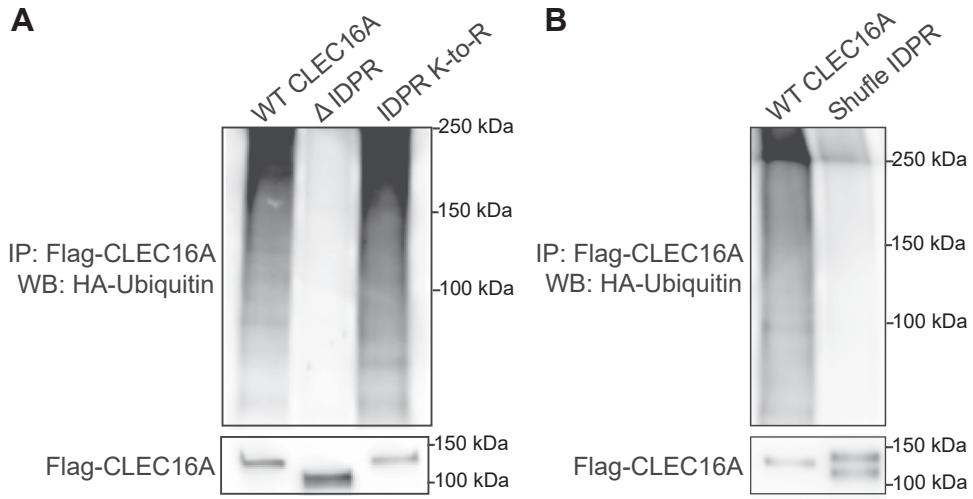

Figure 3. The CLEC16A internal IDPR is not a site of self-ubiquitination but is required for ubiquitin ligase activity. *A*, *in vitro* ubiquitination assay with recombinant CLEC16A-6xHis-Flag WT, ΔIDPR, or IDPR KR. Representative WB and immunoprecipitation (IP) following incubation with ATP, HA-Ubiquitin, E1, and the E2 conjugating enzyme UBE2D3 at 37 °C for 1 h. n = 3/group. *B*, *in vitro* ubiquitination assay with recombinant CLEC16A-6xHis-Flag WT and Shuffle IDPR. Representative WB and IP following incubation with ATP, HA-Ubiquitin, E1, and the E2 conjugating enzyme UBE2D3 at 37 °C for 1 h (n = 3/group). IDPR, intrinsically disordered protein region.

(Fig. 3*A*). Thus, while the internal IDPR appears to support CLEC16A ubiquitin ligase activity, it does not appear to be a site for CLEC16A self-ubiquitination *in vitro*.

RNF41-mediated turnover of CLEC16A depends on lysine residues and amino acid sequence order within the internal CLEC16A IDPR

As CLEC16A does not self-ubiquitinate its own internal IDPR *in vitro*, we speculated that other proteins might act on the internal IDPR to destabilize CLEC16A. CLEC16A forms and stabilizes a tripartite mitophagy regulatory complex with the E3 ubiquitin ligase RNF41 and the deubiquitinase USP8, which together regulate mitophagy through control of Parkin (PRKN) (2, 8, 9). Specifically, CLEC16A directly binds and stabilizes RNF41 through nondegradative ubiquitination (2, 8). Indeed, we have previously shown that CLEC16A physically interacts with and ubiquitinates RNF41, and these actions do not require RNF41 ubiquitin ligase activity (8, 10). RNF41 has a reciprocal regulatory relationship with its fellow partner USP8, wherein USP8 de-ubiquitinates and stabilizes RNF41 and in turn RNF41 ubiquitinates and destabilizes USP8 (39, 40). Building upon knowledge that CLEC16A stabilizes RNF41, we hypothesized that RNF41 may have a similar reciprocal relationship with CLEC16A as with USP8 and thus may destabilize CLEC16A.

We first investigated whether RNF41 acts upon CLEC16A. We found that overexpressing RNF41 resulted in decreased levels of CLEC16A protein (Fig. 4*A*). However, a ligase-dead RNF41 mutant harboring point mutations within the RING domain (C34S and H36Q, hereafter known as CSHQ (41)) did not reduce CLEC16A levels (Fig. 4*A*). This result suggested that RNF41 ubiquitin ligase activity is required for CLEC16A turnover (Fig. 4*A*). Overexpressing RNF41 was also found to increase CLEC16A ubiquitination, whereas this effect was not observed upon overexpressing the ligase-dead mutant (Fig. 4*B*). Further, we found that the function of CLEC16A to stabilize RNF41 required the RNF41 C-terminal substrate binding (Fig. S2) (40). Together, these results implicate a role for RNF41 in the ubiquitination and destabilization of CLEC16A, supporting a reciprocal regulatory relationship between these proteins (Fig. 4*C*).

Given the importance of the internal IDPR to CLEC16A stability, we investigated whether RNF41 acts upon the internal IDPR of CLEC16A. While overexpressing RNF41 led to reduced levels of WT CLEC16A as expected, shuffling or truncating the internal IDPR prevented RNF41 from reducing CLEC16A protein levels (Fig. 4*D*). Further, overexpression of a dominant negative RNF41 lacking its RING domain (dnRNF41) to inhibit RNF41 action led to an elevation in the levels of WT CLEC16A, but this did not occur following truncation of the internal IDPR (Fig. 4*E*). These results suggest that RNF41 acts upon the CLEC16A internal IDPR to destabilize CLEC16A and that this action depends upon the CLEC16A IDPR amino acid sequence order. Notably, overexpression of dnRNF41 did not raise levels of WT CLEC16A to the same degree as CLEC16A lacking the internal IDPR, suggesting that there are additional regulators of CLEC16A stability beyond RNF41 (Fig. 4*E*). Moreover, RNF41 also did not reduce levels of the ubiquitination-resistant CLEC16A internal IDPR mutant (IDPR K-to-R), suggesting that CLEC16A internal IDPR lysine residues are vital for RNF41 to destabilize CLEC16A (Fig. 4*D*).

After determining that RNF41 promotes the ubiquitination and destabilization of CLEC16A in a manner that is dependent on the CLEC16A IDPR amino acid sequence order and its lysine residues, we questioned whether lysine positioning within the CLEC16A IDPR is sufficient for RNF41 to destabilize CLEC16A. Initially, we hypothesized that RNF41 would reduce levels of the CLEC16A construct that retained original lysine positioning but shuffled the remainder of the IDPR (Shuffle IDPR Retain K) because this construct had similar levels and stability to WT CLEC16A (Fig. 2, *E* and *F*). However, overexpressing RNF41 did not reduce levels of the CLEC16A Shuffle IDPR Retain K construct (Fig. 4*D*). This result suggests that while RNF41 requires the lysine residues within the internal IDPR to destabilize CLEC16A, the position of these lysines alone is not sufficient for RNF41 to promote the turnover of CLEC16A. Instead, RNF41-mediated turnover of CLEC16A requires the internal IDPR to have both lysine residues in the correct positions and intact amino acid sequence order.

The CLEC16A internal IDPR promotes the assembly of the CLEC16A–RNF41–USP8 mitophagy regulatory complex

We previously showed that CLEC16A directly binds and ubiquitinates RNF41 to promote the assembly of the CLEC16A–RNF41–USP8 complex (8, 10). We next evaluated whether the putative CLEC16A internal IDPR affects the formation of the CLEC16A–RNF41–USP8 mitophagy complex. Truncating the CLEC16A internal IDPR, or shuffling its residues, reduced CLEC16A binding and ubiquitination of RNF41 compared to WT CLEC16A, following overexpression of the similar protein levels of CLEC16A (Fig. 5*A*). Mutating the CLEC16A internal IDPR also impaired assembly of the tripartite mitophagy complex, as we found reduced binding between CLEC16A and RNF41 as well as RNF41 and USP8 (Fig. 5*B*).

We next questioned how the internal CLEC16A IDPR contributes to RNF41-CLEC16A binding, because the reduced RNF41-CLEC16A binding following IDPR deficiency could be due to either consequent changes in the overall CLEC16A conformation or the loss of a specific RNF41-binding site. IDPRs commonly mediate protein–protein interactions, as their flexible nature makes them amenable for recognizing multiple partners (42). Indeed, overexpression of the CLEC16A internal IDPR fragment alone (AA 347–472; IDPR1 only) was sufficient to bind RNF41 (Fig. 5*C*). Thus, the CLEC16A internal IDPR supports the interaction between CLEC16A and RNF41, in addition to its role as a site for reciprocal control of RNF41 on CLEC16A stability.

An internal IDPR within CLEC16A is validated through biochemical and biophysical assays

Our biochemical studies of the putative internal IDPR of CLEC16A find molecular functions consistent with an IDPR, including control of partner binding, ubiquitin ligase activity,

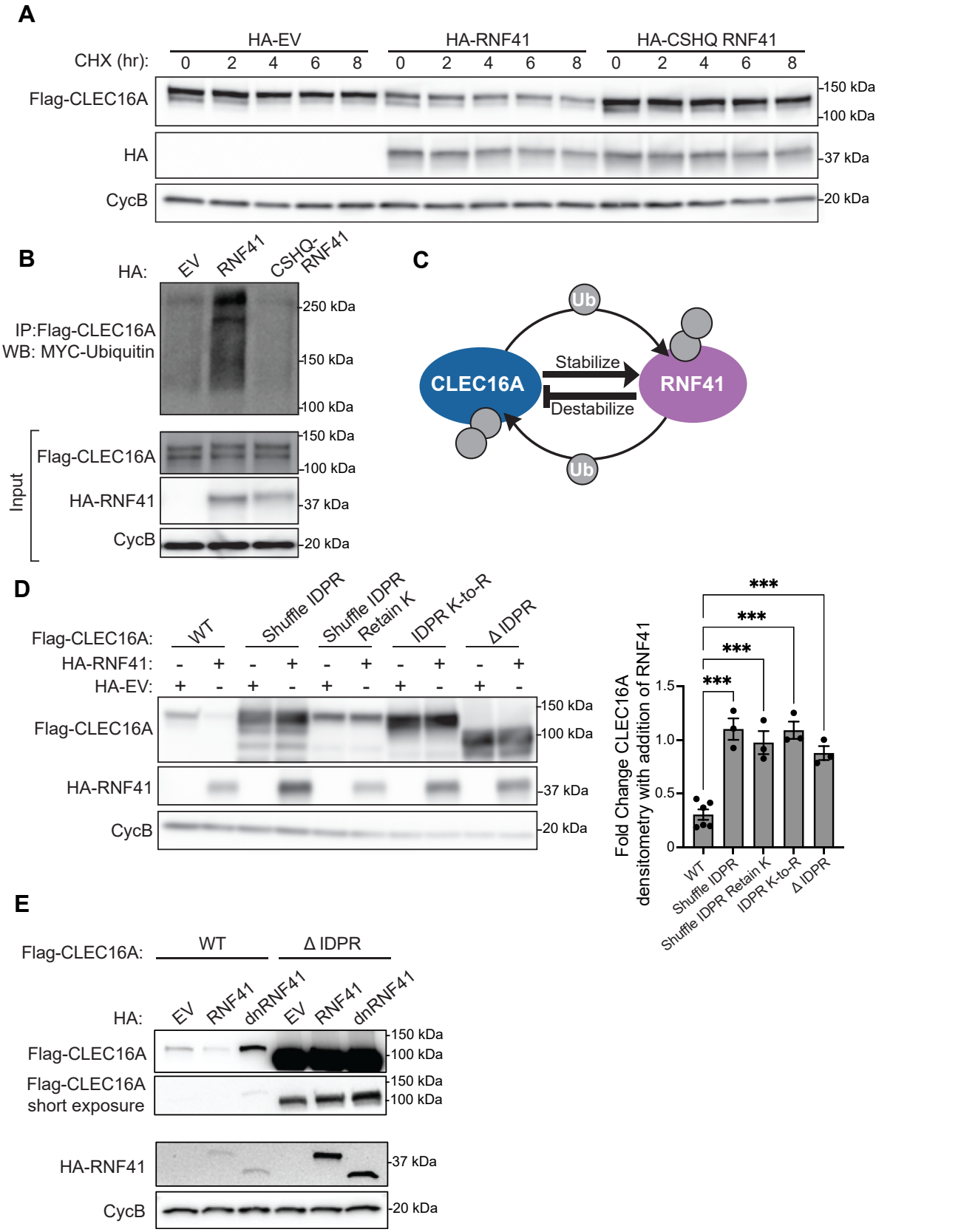

Figure 4. RNF41-mediated turnover of CLEC16A depends on lysine residues and their sequence positioning within the internal IDPR of CLEC16A. *A*, representative WB of Flag-CLEC16A and either HA-EV, HA-RNF41, or HA-CSHQ RNF41 (ligase-dead mutant) transfected into HEK293T cells and treated with cycloheximide (CHX; 300 μg/ml) for 0 to 6 h. n = 3/group. *B*, representative WB of cell-based ubiquitination assay with overexpressed Flag-tagged CLEC16A and MYC-Ubiquitin cotransfected with either HA-EV, HARNF41, or HA-CSHQ RNF41 performed in HEK293T. Cells were treated with 10 μM MG132 for 12 h (n = 3/group). *C*, schematic of proposed reciprocal regulation between CLEC16A and RNF41. *D*, representative Flag WB of WT, Shuffle IDPR, Shuffle IDPR

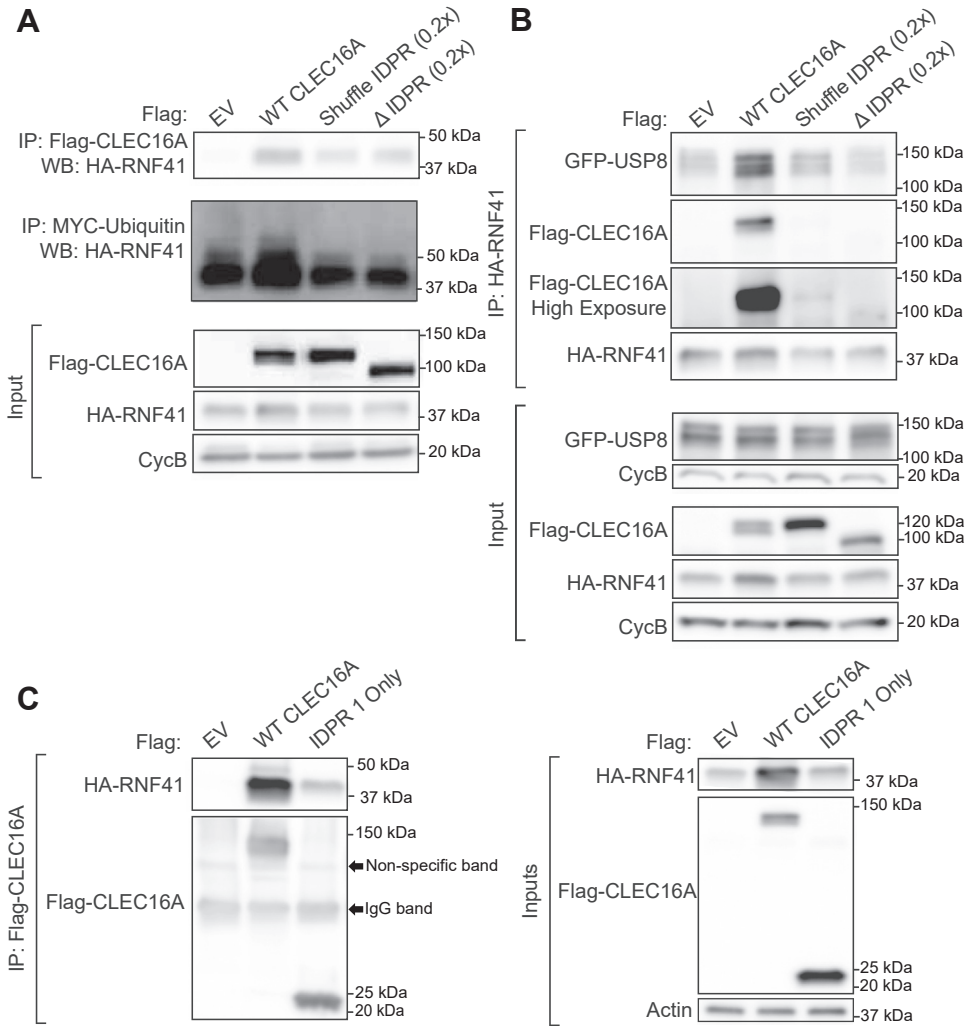

Figure 5. The CLEC16A internal IDPR promotes the assembly of the CLEC16A–RNF41–USP8 mitophagy complex. *A*, representative WBs following IP for Flag-CLEC16A and MYC-Ubiquitin from HEK293T cells transfected with plasmids encoding HA-RNF41, MYC-Ubiquitin, and either Flag-EV, WT, Shuffle IDPR, or ΔIDPR CLEC16A. Shuffle IDPR and ΔIDPR CLEC16A plasmids were transfected at 0.2× that of WT CLEC16A (supplemented with Flag-EV vector to equalize the amount of transfected DNA) to normalize protein levels to that of WT CLEC16A (n = 3/group). *B*, representative WB following IP for HA-RNF41 in HEK293T cells transfected with HA-RNF41, GFP-USP8, and either Flag-EV, WT (1×), Shuffle IDPR (0.2×), or ΔIDPR (0.2×) CLEC16A. Shuffle IDPR and ΔIDPR CLEC16A plasmids were transfected at 0.2× that of WT CLEC16A (supplemented with Flag-EV vector to equalize the amount of transfected DNA) to normalize protein levels to that of WT CLEC16A (n = 3/group). *C*, representative WB following IP for Flag-CLEC16A in HEK293T cells transfected with HA-RNF41 and either Flag-EV, WT CLEC16A, or CLEC16A IDPR1 only (AA 347–472) (n = 3/group). IDPR, intrinsically disordered protein region.

and protein turnover. These findings motivated us to experimentally investigate the presence of an internal IDPR in CLEC16A. IDPRs characteristically demonstrate slow migration in SDS-polyacrylamide gels due to their expanded nature and greater number of charged residues which leads to weak binding to SDS (26, 43). Full-length WT CLEC16A and the CLEC16A ΔIDPR mutant migrated at their expected molecular mass (Fig. 6*A*). However, the internal CLEC16A putative IDPR alone (AA 347–472) migrated a shorter distance than what is expected, visualized as a band ∼1.6-times greater than the expected size, consistent with an IDPR (Fig. 6*A*).

We next investigated the structural conformation of the putative CLEC16A IDPR using NMR. IDPRs lack secondary structure, and the hydrogen atoms within their backbone all exist in a similar chemical environment, resulting in uniform clustering in the hydrogen dimension of a ^{1}H-^{15}N heteronuclear single quantum coherence-NMR spectra (44). Notably, the heteronuclear single quantum coherence-NMR spectra of the CLEC16A putative internal IDPR was tightly clustered near 8 ppm, supporting the hypothesis that CLEC16A contains an internal IDPR (Fig. 6*B*).

To confirm the CLEC16A internal region is an IDPR, we next investigated whether features of secondary structure were present. While the CLEC16A internal putative IDPR was not amenable to secondary structure characterization *via* carbon-detect NMR due to poor carbon-detect spectral quality and

retain K, IDPR K-to-R, and ΔIDPR CLEC16A cotransfected with HA-EV or HA-RNF41 in HEK293T cells. Densitometry represents fold change in protein levels per construct following the addition of RNF41, normalized to Cyc B. No significant differences were found between CLEC16A Shuffle IDPR, Shuffle IDPR Retain K, IDPR K-to-R, and ΔIDPR following the addition of RNF41 (n = 3–6/group). *E*, representative Flag WB of WT and ΔIDPR CLEC16A cotransfected with HA-EV, HA-RNF41, or HA-dnRNF41 in HEK293T cells. (n = 3/group). ***$p < 0.001$. IDPR, intrinsically disordered protein region.

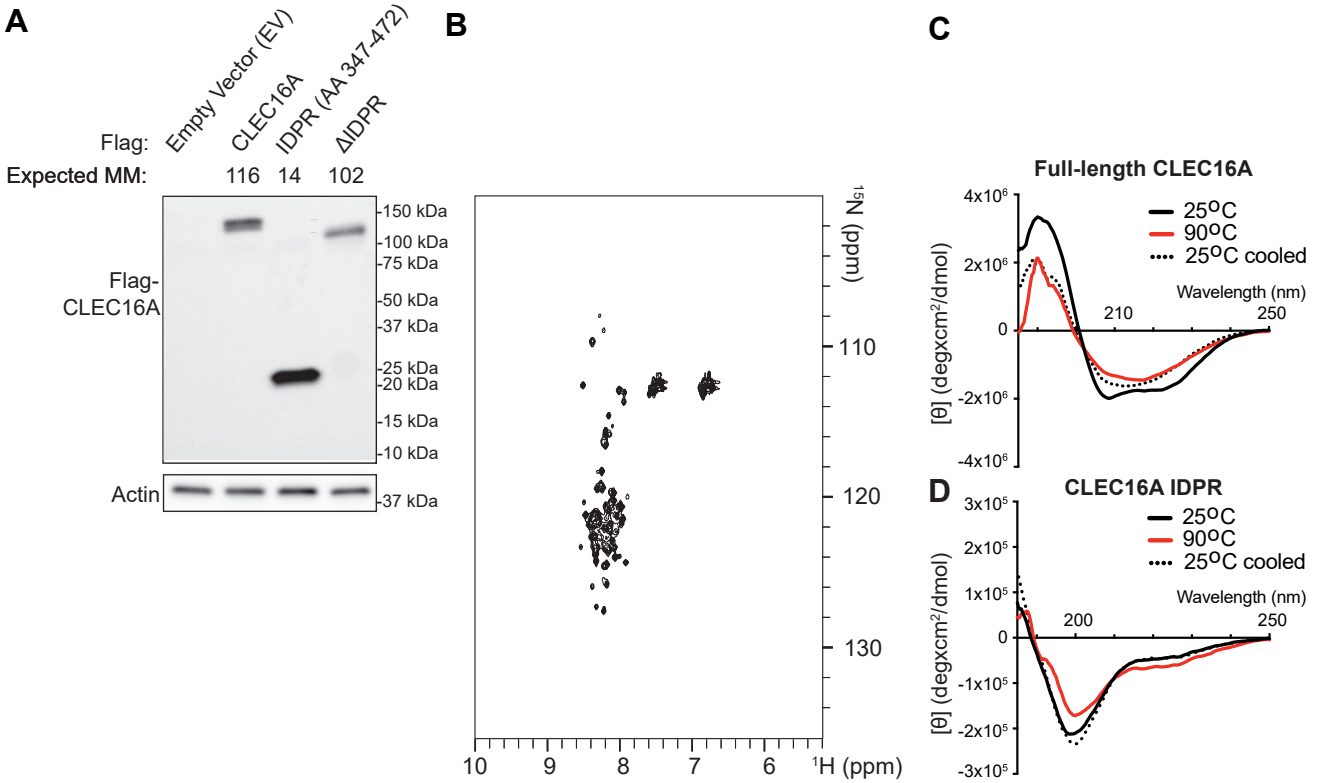

Figure 6. Experimental confirmation of the CLEC16A internal IDPR using biochemical and biophysical approaches. *A*, representative WB in HEK293T cells transfected with Flag-CLEC16A constructs (full-length CLEC16A, CLEC16A internal IDPR only (AA 347–472), or CLEC16A ΔIDPR). Beta actin is included as a loading control (n = 3/group). *B*, ^{1}H-^{15} N HSQC spectra of recombinant CLEC16A internal IDPR (AA 347–472). Spectra clusters near ^{1}H 8 ppm, consistent with being an IDPR. *C*, CD spectra of recombinant full-length (WT) mouse CLEC16A. Line represents the average of three reads. Reads were taken of sample at 25 °C (*black solid line*), then after heating to 90 °C (*red line*), then after cooling back to 25 °C (*black dashed line*). Spectra indicates secondary structure is present. *D*, CD spectra of recombinant CLEC16A internal IDPR (AA 347–472), performed as noted in panel (C). Spectra indicate that secondary structure elements are absent, consistent with an IDPR. HSQC, heteronuclear single quantum coherence; IDPR, intrinsically disordered protein region.

overlapping NMR peaks, we instead used far-UV CD spectroscopy to probe secondary structure. Classically, CD spectra of alpha helices exhibit two minima, one at 208 nm with a deeper second minimum at 220 nm, CD spectra of beta-sheets exhibit a single minimum at 218 nm, and unstructured peptides/IDPRs exhibit a single minimum around 200 nm (45). The CD spectra obtained for recombinant full-length CLEC16A contained minima at 208 nm and 220 nm, consistent with the largely alpha-helical structure predicted by AlphaFold (Figs. 6*C* and 1*A*). Conversely, the CD spectra of the putative internal CLEC16A IDPR had a single minimum near 200 nm, in line with lack of secondary structure (Fig. 6*D*) (45, 46). Further, while heating full-length CLEC16A irreversibly disrupted its alpha-helical secondary structure, heating the internal CLEC16A fragment did not substantially change its spectral features (Fig. 6, *C* and *D*). This result confirmed that the internal CLEC16A fragment lacks secondary structure and is indeed an IDPR (Fig. 6, *C* and *D*). Taken together, these orthogonal biophysical techniques experimentally validate the presence of an IDPR within the internal domain of CLEC16A.

Discussion

We identify an internal IDPR in CLEC16A that regulates reciprocal CLEC16A–RNF41 interactions. Loss of the CLEC16A internal IDPR impairs assembly of the tripartite CLEC16A–RNF41–USP8 mitophagy complex, as CLEC16A had reduced ability to bind and ubiquitinate RNF41 (Fig. 5). The internal IDPR regulates CLEC16A turnover (Fig. 2), at least in part due to ubiquitination of IDPR lysine residues by RNF41 (Fig. 4). To the best of our knowledge, our studies identify RNF41 as the first known protein to regulate CLEC16A stability. Together, we assemble an intricate understanding of the importance of an IDPR in CLEC16A, which is a key regulator of human disease pathogenesis.

Our studies uncover a novel RNF41-CLEC16A reciprocal regulatory relationship that is mediated by the internal IDPR of CLEC16A. Our observations implicate an additional layer in the tight regulatory balance of the upstream mitophagy regulatory machinery of CLEC16A, RNF41, and USP8 that ultimately regulate PRKN. RNF41 is a previously identified CLEC16A partner and is implicated in reciprocal regulation of other partners including USP8 (8, 39, 40). USP8 deubiquitinates and stabilizes RNF41 (40), while RNF41 in turn ubiquitinates and destabilizes USP8 (39). Our previous and current studies find a similar regulatory relationship between RNF41 and CLEC16A, whereby we previously showed that CLEC16A stabilizes RNF41 by nondegradative ubiquitination (2, 8, 10), and here we find that RNF41 reciprocally promotes CLEC16A ubiquitination and turnover. Further, CLEC16A

stabilizes RNF41 to mediate PRKN proteasomal degradation, primarily during states of optimal metabolic health (2, 10). Following mitochondrial damage, USP8 will de-ubiquitinate PRKN at K6 linkages to promote mitochondrial localization of PRKN and activate mitophagy (47). Mitochondrial quality control is tightly tuned, activated following mitochondrial damage to clear sick/unhealthy mitochondria, while remaining at lower levels during times of optimal mitochondrial health (10, 48). We presume that the cross-regulatory control of both CLEC16A and USP8 by RNF41 allows the mitochondrial quality control regulatory machinery upstream of PRKN the flexibility to modulate the activation or repression of mitophagy on demand. Uncovering a reciprocal regulatory relationship between CLEC16A and RNF41, similar to that between USP8 and RNF41, emphasizes the complex relationships that govern this tripartite complex. These studies may also position RNF41 in a more central role in mitophagy than previously appreciated, as it can lead to the degradation of all of these key mitophagy regulators (CLEC16A, USP8, and PRKN; (39, 49)). It will be intriguing to clarify how the response to mitochondrial stress/damage may modulate the reciprocal balance of CLEC16A-RNF41 that we describe in this work, as well as the broader effects on mitophagy overall (including USP8 and PRKN).

Our work finds that the internal CLEC16A IDPR bears opposing functions compared to the CLEC16A C-terminal IDPR we described recently in separate work (see model in Fig. 7) (14). The internal IDPR destabilizes CLEC16A, in contrast to the C-terminal IDPR that promotes CLEC16A stability (Fig. 7). While the internal CLEC16A IDPR mediates CLEC16A turnover in a manner that depends on the presence of its lysine residues, the C-terminal CLEC16A IDPR oppositely prevents CLEC16A turnover by reducing self-ubiquitination. The C-terminal CLEC16A IDPR depends upon its proline residues, rather than lysine residues, to stabilize CLEC16A. While the internal CLEC16A IDPR is required for CLEC16A-RNF41 binding within the mitophagy complex, the C-terminal CLEC16A IDPR is dispensable for RNF41 binding. Finally, while the internal IDPR may contribute to CLEC16A ubiquitin ligase activity through an undetermined mechanism, the C-terminal IDPR does not contribute to ubiquitin ligase activity. Together, we find that the two IDPRs within CLEC16A play very distinct and often opposing roles, expanding our knowledge on the variety of molecular functions for IDPRs, even within a single protein. Future studies are needed to determine how these unique IDPRs balance their opposing actions to control CLEC16A stability and function.

There is controversy over whether the function of IDPRs depends on amino acid sequence order and composition (31, 32). While CLEC16A is highly conserved in mammals, the internal IDPR overlaps with a region of lower relative conservation (Fig. S1), and we questioned the importance of the IDPR amino acid sequence to its function. However, our

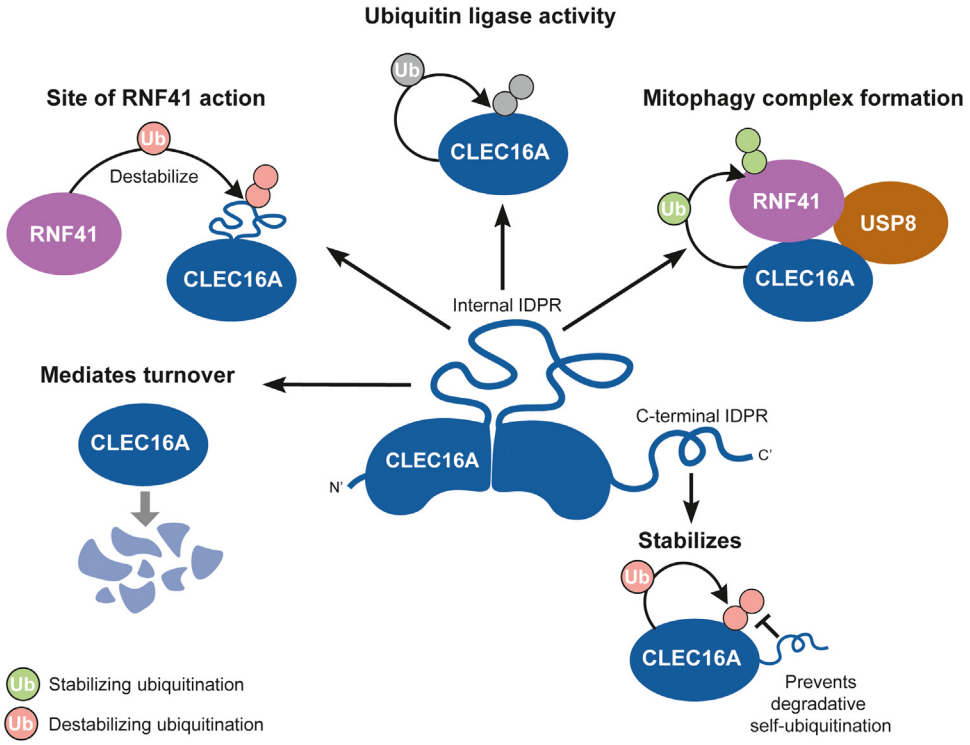

Figure 7. Proposed model for CLEC16A IDPRs' contributions to its molecular functions and reciprocal regulation by RNF41. The C-terminal IDPR of CLEC16A is known to enhance CLEC16A stability by preventing self-ubiquitination, whereas the functions of the internal IDPR were unknown until the present work. The internal IDPR is critical for the enzymatic function and molecular interactions of CLEC16A. This internal IDPR regulates CLEC16A turnover and is the site by which RNF41 acts to destabilize CLEC16A. The internal IDPR of CLEC16A is also required for its E3 ligase activity, and the loss of this disordered region impairs both self-ubiquitination and the ability of CLEC16A to ubiquitinate RNF41. The internal IDPR binds to RNF41 and mediates the assembly of the CLEC16A–RNF41–USP8 mitophagy complex. IDPR, intrinsically disordered protein region.

studies demonstrate that the amino acid sequence order of the internal IDPR of CLEC16A is indeed important for its function. Disrupting the order of residues within the CLEC16A internal IDPR through random shuffling prevents its turnover and prevents RNF41 action upon CLEC16A, indicating these roles are sequence dependent. Lysine residues within the CLEC16A internal IDPR are required for both CLEC16A turnover and for RNF41 to act upon CLEC16A, which aligns with the known enrichment of degradative ubiquitination sites within IDPRs (37, 50). We initially hypothesized that returning lysines to their original position after shuffling the internal IDPR (Shuffle IDPR retain K) may restore CLEC16A turnover and RNF41 action upon CLEC16A, due to the similarities between the CLEC16A construct with a shuffled IDPR and the construct lacking lysine residues (Fig. 2, *C*, *E*, and *F*). However, the levels and stability of the Shuffle IDPR retain K CLEC16A construct were actually slightly elevated relative to that of WT CLEC16A (Fig. 2, *E* and *F*). This may be explained by the inability of RNF41 to promote turnover of this CLEC16A construct, where the lysines of its internal IDPR are in their native positions yet the remaining sequence order is perturbed. Thus, for RNF41 to destabilize CLEC16A, the internal IDPR must have correctly positioned lysines, as well as an intact amino acid sequence surrounding the lysines.

IDPRs often contain short linear motifs (∼2–5 residues) that serve as molecular recognition sites for partner proteins (51–55). We speculate that the internal IDPR of CLEC16A may contain an unidentified short linear motif that mediates interaction with RNF41. Lysines can serve as important degron motifs, and it is also possible the pattern and position of lysine residues within the IDPR of CLEC16A plays a role in its recognition and degradation by RNF41 or other partners (37, 38). Future studies may focus on identifying putative motifs within the IDPR of CLEC16A and determining if retaining such a motif is sufficient for CLEC16A turnover and function.

IDPRs within E3 ubiquitin ligases control many functions including protein localization and trafficking, conformation, enzymatic activity, and substrate binding (20, 21, 56). We found the internal IDPR within CLEC16A may have a dual role in promoting both its binding to partners/substrates and its enzymatic activity (Fig. 7). The flexibility of IDPRs can regulate ubiquitin ligase enzymatic activity by controlling ubiquitin transfer and processivity (20, 21). For example, E3 ligases in the single-RING finger family such as CBL have a flexible IDPR linker that connects a substrate-binding domain and E2-binding domain (20, 21). The flexible linker in CBL allows the E2 ubiquitin-conjugating enzyme to be brought towards the substrate for processive substrate ubiquitination (20, 21). Additionally, IDPRs in E3 ligases contribute to partner and substrate interactions, as increasingly disordered ligases have more partners (21). The substrate-binding domains of E3 ligases are also more disordered when compared to their other domains (21). We found the internal CLEC16A IDPR promotes the binding and ubiquitination of RNF41 and may also support CLEC16A ubiquitin ligase activity. Loss of the CLEC16A internal IDPR impairs RNF41 ubiquitination (Fig. 5*A*), yet this may stem solely from reduced binding and thus reduced proximity. However, disrupting the CLEC16A internal IDPR also reduced its self-ubiquitination *in vitro* (Fig. 3*A*), suggesting this IDPR could have a dual role in both enzymatic activity and substrate binding. However, our mechanistic and molecular understanding of how CLEC16A functions as a ubiquitin ligase, how the IDPR may support its ligase activity or the specific CLEC16A IDPR lysine residues and ubiquitin linkages involved in these processes, remains largely unclear and is of great interest for future work.

Our studies describe the molecular function of an IDPR in the disease-associated protein CLEC16A, which may provide avenues to therapeutically target CLEC16A. We found that the CLEC16A internal IDPR regulates CLEC16A turnover, and multiple human diseases are associated with reduced CLEC16A levels (2, 14, 57). For example, genetic variants that decrease *CLEC16A* expression in human islets are associated with reduced human β-cell function, dysglycemia, and increased T1D risk (2). Additionally, a CLEC16A isoform that lacks the C terminus associated with multiple sclerosis is less stable than the full-length CLEC16A but otherwise appears functional in ubiquitin ligase activity and partner binding (14, 57). By identifying an IDPR within CLEC16A that regulates its turnover, our work lays the foundation for therapeutic approaches to block access to this region and prevent CLEC16A turnover, thus increasing protein levels to potentially enhance CLEC16A function to treat or prevent disease.

Experimental procedures

Protein expression and purification

Recombinant protein was generated according to previous protocols (14). To generate recombinant CLEC16A AA 347-472, a pMCSG7-CLEC16A 347-472 TEV-6xHis expression plasmid was transformed into Rosetta2 cells. Transformed cells were cultured in 10 ml LB overnight, then transferred to 1 l of LB, and grown at 37 °C until an optical density of 600 nm was reached. Bacteria were pelleted and washed, then resuspended in 1 l of minimal medium (12 g/l K_2HPO_4, 9 g/l KH_2PO_4, 1 g/l $^{15}NH_4Cl$, 2.5 g/l NaCl, 25 mg/l thiamine HCl, 4 g/l ^{13}C-glucose, 0.5 g/l $MgSO_4$, 0.1 g/l NaOH) that was supplemented with 1 ml of 100 mM $CaCl_2$, 1 ml of Metal Solution (0.3 g/65 ml $FeSO_4{\cdot}7H_2O$, 0.2 g/65 ml $ZnSO_4{\cdot}7H_2O$, 0.4 g/65 ml $CoCl_4{\cdot}6H_2O$, 0.3 g/65 ml $(NH_4)_6Mo_7O_{24}{\cdot}4H_2O$, 0.3 g/65 ml $CuSO_4$, 0.2 g/65 ml $MnCl_4{\cdot}4H_2O$, 0.1 g/65 ml H_3BO_3), and ampicillin, as done previously (14). CLEC16A expression was induced with IPTG (Agilent, 300127) overnight at 20 °C. Pelleted bacteria were freeze/thawed at −80 °C. The pellet was sonicated in lysis buffer (1× PBS [Fisher, BP399-20], 1% CHAPS [Sigma Aldrich, C9426], 10 mM $MgCl_2$, 2 μl benzonase [25 U/μl; Millipore, 71206]) with added protease inhibitor (Thermo Fisher Scientific, PIA32965). The 6xHis-tagged protein was purified on a nickel column (Qiagen, 30250; Ni-NTA Agarose). Protein was eluted in 300 mM imidazole in 1× PBS, then incubated with TEV protease (NEB, P8112S) at 4 °C overnight in 0.1% BME in 1× PBS. A nickel column then removed cleaved 6xHis tag. The

protein was purified from the eluate with Q anion exchange chromatography (AKTAAxpress, GE Healthcare). Fractions were visualized on SDS-PAGE, and those containing the peptide of interest were subjected to size-exclusion chromatography (AKTA Purifier 10). SDS-PAGE was used to visualize fractions, and those containing the peptide were dialyzed into 50 mM sodium cacodylate, 150 mM NaCl, pH 6.5 in ddH_2O for NMR.

Recombinant protein for CD was generated using the pFLAG-CMV-5a-6xHis expression plasmid containing either CLEC16A or the CLEC16A internal fragment (AA 347–472). The same protocol as above was followed, except transformed cells were not washed and resuspended into minimal medium. Protein fractions for CD were dialyzed into 10 mM potassium phosphate, 50 mM Na Fluoride pH 7.5 in ddH_2O. All proteins were concentrated prior to use.

Recombinant protein used in *in vitro* ubiquitination assays was generated by the expression of 6xHis-tagged protein in 293T cells. Protein was purified with a nickel agarose gravity column (Ni-NTA agarose) according to manufacturer's instructions.

Nuclear magnetic resonance

NMR was performed as previously described (14). The $^{13}C/^{15}N$ CLEC16A internal peptide fragment (AA 437–472) was prepared as described above in a buffer of 50 mM sodium cacodylate, 150 mM NaCl. D_2O (10%) was added to the sample, and the sample was loaded in a Shigemi NMR Tube (Wilmad-LabGlass, SP Scienceware, BMS-005B). NMR was performed with an 18.8 T Bruker Ascend magnet equipped with Bruker NEO spectrometer operating at ^1H frequencies of 800.25 MHz. The spectrometer was equipped with an inverse TCI cryoprobe. The NMR spectra were collected at 298K. All data were processed in Topspin 4.0.9 software (https://www.bruker.com/en/products-and-solutions/mr/nmr-software/topspin.html) and converted to Sparky format for analysis and visualization.

We first collected ^1H-^{15}N HMQC spectra of the CLEC16A internal fragment (AA 347–472) with a matrix size of 2048 × 512, spectral width of 15.32 ppm (^1H) x 36 ppm (^{15}N), and eight scans, totaling an acquisition time of 23 min. We attempted chemical shift assignments and secondary structure analyses using standard C′ detect NMR methods (29). However, due to the weak signal obtained from the (H^{α}-start) ^{15}N-^{13}C CON collected, this sample was not suitable for chemical shift assignments as done previously (29).

Circular dichroism

Far-UV CD was performed using the JASCO J-815 spectrometer. Samples were prepared in 10 mM potassium phosphate, 50 mM Na Fluoride pH 7.5 in ddH_2O as described above. A 10-mm pathlength cuvette was used. Measurements were taken from 180 nm to 400 nm, at 0.5-nm increments. The high tension voltage was monitored to ensure the collected data was in the dynamic range of measurement. Each CD trace represents the average of three independent reads. Samples for far-UV CD spectra were obtained at 25 °C, then after heating to 90 °C, and again after cooling to 25 °C.

Cell culture, transfections, and treatments

293T cells were grown in DMEM (Gibco, 11965) that was supplemented with 10% Fetal-Plex (Gemini Bio Products, 50-753-2987), 1 mM sodium pyruvate (Thermo Fisher Scientific, 11-360-070), and 50 units/ml penicillin-streptomycin (Thermo Fisher Scientific, 15140-122). Cells were transfected with Lipofectamine 2000 according to the manufacturer's protocol (Thermo Fisher Scientific, 11668027). Cells were treated with dimethylsulfoxide (Thermo Fisher Scientific, BP231-100) and cycloheximide (EMD, 239-765).

Antibodies

All antibodies used are listed in Table S1.

Plasmids

Constructs for mammalian overexpression studies included the pFLAG-CMV-5a-CLEC16A WT (2), pFLAG-CMV-5a-CLEC16A WT-6xHis (2), pcDNA3.1 3x-HA-RNF41/Nrdp1 (2), pcDNA3.1 3x-HA-CSHQ-RNF41/Nrdp1 (2), and MYC-ubiquitin (48, 58). Plasmids with CLEC16A internal IDPR mutations (AA 347–472) for mammalian cell overexpression studies were generated by gene synthesis into pBluescriptSK(+) (Biomatik, custom order) that were subsequently subcloned into pFLAG-CMV-5a by restriction digest and ligation. These included the CLEC16A ΔIDPR, Shuffle IDPR, IDPR K-to-R, and Shuffle IDPR retain K construct. The randomly shuffled internal IDPR CLEC16A construct was generated using a random shuffling algorithm, and PROSITE and SMART domain prediction tools confirmed that no new domains were introduced (33, 34, 59). The IDPR K-to-R construct mutated the 15 lysine residues to arginines within CLEC16A region spanning residues 347 to 472. The Shuffle IDPR retain K construct was designed by taking the Shuffle IDPR amino acid sequence and returning the lysine residues to their original position within the sequence while leaving the remaining amino acids shuffled. The amino acid sequences for these constructs are as follows:

WT CLEC16A AA 347 to 472 (internal IDPR):

PAQDVPRSSAKPSIRCFIKPTETLERSLEMNKHKGKKRM
QKRPNYKNVGEEEDEERGSAEDAQEDAEKTKGTEGGSKS
MKTSGEREEIEMVIMKLGKLSEVAAAGTSVQEQNTTDEE
KSAATNSEN

Shuffle IDPR:

MARDKMESNNKTSACSEITGEPETQASREQKVDESEQA
EKTDGPNDEMSEAIVAKVLRKNVKKPFKKTREEELLKMN
MGASRITNQHKKAYSSLGEEPIGGEARRKGESAPETEKDG
EETGSQSTV

IDPR K-to-R:

PAQDVPRSSARPSIRCFIRPTETLERSLEMNRHRGRRRM
QRRPNYRNVGEEEDEERGSAEDAQEDAERTRGTEGGSRS
MRTSGEREEIEMVIMRLGRLSEVAAAGTSVQEQNTTDEE
RSAATNSEN

Shuffle IDPR retain K:

MARDMESNNTKSACSEITKGEPETQASREQVKDKEKKS EQKAETDKGPNDEMSEAIVAVLRNVPFTRKEKEELLMNK MGKASRITNQHAYSSLKGEKEPIGGEARRGESAPETEDGE KETGSQSTV

Plasmids that were used to express recombinant protein for *in vitro* ubiquitination assays and CD studies include the previously generated pFLAG-CMV-5a-CLEC16A WT-6xHis (2). For CD, the pFLAG-CMV-5a-6xHis CLEC16A internal IDPR only (AA 347–472) was generated by PCR amplifying the internal CLEC16A IDPR into pCR-BLUNT II TOPO backbone (Zero blunt TOPO cloning kit; Invitrogen, 450245), followed by sequence validation. The fragment was then ligated into pFLAG-CMV-5a and subcloned *via* restriction digest and ligation into pFLAG-CMV-5a-6xHis. For *in vitro* ubiquitination studies, the pFLAG-CMV-5a-6xHis ΔIDPR, IDPR K-to-R, and Shuffle IDPR CLEC16A constructs were generated by restriction digest of the corresponding pFLAG-CMV-5a plasmid and ligation into the pFLAG-CMV-5a-6xHis plasmid.

To generate the recombinant CLEC16A internal peptide fragment AA 347 to 472 for NMR, this fragment was amplified using PCR from pFLAG-CMV-5a-CLEC16A (WT) (2). Primers with ligation-independent cloning sites were used (Forward- 5′ TACTTCCAATCCAATGCTCCTGCACAGGA TGTTCCC 3′ and Reverse- 5′ TTATCCACTTCCAATGT-TAATTCTCTGAGTTCGTGGCG 3′). The PCR product was annealed with a linearized pMCSG7 bacterial plasmid (gifted from the Center for Structural Biology, University of Michigan) which has an N-terminal TEV-cleavable 6xHis tag. The plasmid was transformed into high efficiency DH5-α competent *Escherichia coli* and confirmed by sequencing.

The pcDNA3.1 3x-HA-RNF41/Nrdp1 truncation constructs were generated by PCR amplifying the fragments into pCR-BLUNT II TOPO backbone (Zero blunt TOPO cloning kit; Invitrogen, 450245), followed by sequence validation. The fragment was then restriction digested and ligated into pcDNA3.1 3x-HA. Primers used are as follows: Δ1-71 (Forward- 5′ GGATCCATGCGGAACATGTTGTCAAAG 3′ and Reverse- 5′ TCTAGATTATATCTCCTCCACACCATG 3′), Δ1-134 (Forward- 5′ GGATCCATTAAGCACCTGCGCTC CGTG 3′ and Reverse- 5′ TCTAGATTATATCTCCTCCA-CACCATG 3′), Δ193-317 (Forward- 5′ GGATCCATGGGG-TATGATGTGACCCGT 3′ and Reverse- 5′ TCTAGATTAT GTCTCCTCCAGGTTCTGAAG 3′). Deletion of initial 71 amino acids at the amino terminus of RNF41 (Δ1–71), subsequently removing the RNF41 RING domain, was also utilized for dnRNF41 studies similar to previous approaches (60, 61).

In vitro *ubiquitination assays*

Ubiquitination of purified recombinant CLEC16A WT-6xHis-Flag and CLEC16A mutants were assessed *in vitro* by incubation of 1 μM CLEC15A-6xHis-Flag, 50 nM E1 cocktail (Bio-Techne E305), 5 μM UBE2D3 (Bio-Techne, E2-627), 50 μM HA-ubiquitin (Bio-Techne, U-110), Mg-ATP (Bio-Techne, B-20), and conjugation reaction buffers for 60 min at 37 °C. Ubiquitinated CLEC16A was detected by performing a Flag immunoprecipitation followed by SDS-PAGE and immunoblot for HA-Ubiquitin.

Western blotting

Cells were lysed in RIPA buffer (50 mM Tris pH 8, 150 mM NaCl, 1% NP-40, 12 mM deoxycholate, 3 mM SDS) with protease and phosphatase inhibitors (Millipore, 539143 and 524,625), followed by sonication. Lysates were centrifuged, and protein concentration was determined (MicroBCA; Pierce, 23235). Equal protein amounts of supernatant were combined with 4× loading dye containing 15 mg/100 μl SDS and run on a 4 to 15% gradient Criterion TGX Gel (BioRad, 567-1084) in Tris-Glycine-SDS running buffer at 150 V. Proteins were transferred to nitrocellulose membranes (BioRad, 1630112) in transfer buffer (25 mM Tris, 200 mM glycine) supplemented with 20% methanol for 90 min at 90 V. Antibodies were incubated with the nitrocellulose membrane in 5% milk in 1× Tris-Buffered Saline, pH 7.5 (15.22 mM Tris–HCl, 4.62 mM Tris-Base, 150 mM NaCl) with 0.05% Tween 20) overnight, followed by incubation with horseradish peroxidase–conjugated secondary antibodies.

Immunoprecipitation

Cells were lysed in NP-40 lysis buffer (150 mM NaCl, 1% NP-40, IGEPAL, 50 mM Tris, pH 8.0) with protease and phosphatase inhibitors (Millipore, 539143 and 524625). The lysate was sheared by passing through a 21-gauge needle. Lysates were clarified by centrifuging and then incubated with either Flag M2 Affinity Gel (Sigma A2220), anti MYC/c-Myc agarose beads (Sigma A7470), or HA agarose beads (Biolegend 900801), rotating at 4 °C overnight. The beads were then rinsed in NP-40 lysis buffer three times. Protein was eluted off the beads in 2× Laemmli buffer (Sigma, S3401) at 70 °C for 10 min. Samples were run on SDS-PAGE.

Homology and evolutionary conservation analyses

The amino acid sequence of select CLEC16A homologs were retrieved from Ensembl, along with the percentage of the homologous sequence matching the human CLEC16A sequence (62). A neighbor-joining phylogenetic tree was constructed using Simple Phylogeny, part of the ClustalW2 package at EMBL-EBI (63, 64). Evolutionary conservation of CLEC16A residues was analyzed with ConSurf, which identifies protein homologs in UniProt using HMMER (65). ConSurf selected 150 sequences for analyses that sampled the list of 264 unique CLEC16A homologs. ConSurf performs multiple sequence alignment and calculates the evolutionary conservation of each residue position using an empirical Bayesian interference.

Statistics

The data are shown as the average value, and error bars represent SEM. Statistical significance was determined using an unpaired two-tailed student's *t* test for comparisons between two groups. For multiple comparisons, statistical significance was determined *via* ANOVA with a

Dunnett's *post hoc* multiple comparisons test. A 5% significance level was used for all statistical tests. All statistical analysis was performed using Prism software (GraphPad software, LLC).

Data availability

All data are contained within the manuscript.

Supporting information—This article contains supporting information (62).

Acknowledgments—Recombinant protein for biophysical studies reported in this publication was generated with supported from the University of Michigan Center for Structural Biology (CSB). The CSB acknowledges support from the U-M Life Sciences Institute, the U-M Rogel Cancer Center, the U-M Medical School Endowment for Basic Sciences, and grants from the NIH. We thank the University of Michigan BioNMR Core fand for assistance performing, analyzing, and interpreting NMR studies. The University of Michigan BioNMR Core is supported by the U-M College of Literature, Sciences and Arts, Life Sciences Institute, College of Pharmacy, and the Medical School along with the U-M Biosciences Initiative. We thank Drs. H. Popelka, P. Arvan, D. Fingar, and members of the Soleimanpour laboratory for helpful advice.

Author contributions—M. A. G. and S. A. S. conceptualization; M. A. G., J. Z., B. C., M. P. V., N. X., V. S., and D. S. investigation; M. A. G., M. P. V., and D. S. formal analysis; M. A. G. data curation; M. A. G. and S. A. S. writing–original draft; M. A. G. and S. A. S. funding acquisition; J. Z., B. C., M. P. V., V. S., N. A. K., D. S., D. J. K., S. S., and S. A. S. writing–review and editing; N. A. K., D. S., D. J. K., S. S., and S. A. S. resources; N. A. K., D. S., D. J. K., S. S., and S. A. S. supervision; S. A. S. visualization.

Funding and additional information—M. A. G. was supported by the NIH (F31-DK-122761, T32-GM-007315, T32-GM-008322). S. A. S was supported by the JDRF (CDA-2016-189, SRA-2018-539, COE-2019-861), the NIH (R01 DK108921, U01 DK127747), the Department of Veterans Affairs (I01 BX004444), the Brehm family, the Anthony family, and a Brehm T1D Pilot and Feasibility Grant from the Michigan Diabetes Research Center (P30-DK020572). S. S. was supported by the JDRF (CDA-2016-189) and NIH (R01 DK108921). The JDRF Career Development Award to S.A.S. is partly supported by the Danish Diabetes Academy and the Novo Nordisk Foundation. D. J. K. was supported by the NIH (GM131919). The content is solely the responsibility of the authors and does not necessarily represent the official views of the National Institutes of Health.

Conflict of interest statement—The authors have declared that no conflict of interest exists.

Abbreviations—The abbreviations used are: IDPR, intrinsically disordered protein region.

References

1. Hakonarson, H., Grant, S. F., Bradfield, J. P., Marchand, L., Kim, C. E., Glessner, J. T., *et al.* (2007) A genome-wide association study identifies KIAA0350 as a type 1 diabetes gene. *Nature* **448**, 591–594
2. Soleimanpour, S. A., Gupta, A., Bakay, M., Ferrari, A. M., Groff, D. N., Fadista, J., *et al.* (2014) The diabetes susceptibility gene Clec16a regulates mitophagy. *Cell* **157**, 1577–1590
3. Jagielska, D., Redler, S., Brockschmidt, F. F., Herold, C., Pasternack, S. M., Garcia Bartels, N., *et al.* (2012) Follow-up study of the first genome-wide association scan in alopecia areata: IL13 and KIAA0350 as susceptibility loci supported with genome-wide significance. *J. Invest. Dermatol.* **132**, 2192–2197
4. Gingerich, M. A., Sidarala, V., and Soleimanpour, S. A. (2020) Clarifying the function of genes at the chromosome 16p13 locus in type 1 diabetes: CLEC16A and DEXI. *Genes Immun.* **21**, 79–82
5. Fujimaki, T., Kato, K., Yokoi, K., Oguri, M., Yoshida, T., Watanabe, S., *et al.* (2010) Association of genetic variants in SEMA3F, CLEC16A, LAMA3, and PCSK2 with myocardial infarction in Japanese individuals. *Atherosclerosis* **210**, 468–473
6. Hafler, D. A., Compston, A., Sawcer, S., Lander, E. S., Daly, M. J., De Jager, P. L., *et al.* (2007) Risk alleles for multiple sclerosis identified by a genomewide study. *N. Engl. J. Med.* **357**, 851–862
7. Yoshida, T., Kato, K., Yokoi, K., Oguri, M., Watanabe, S., Metoki, N., *et al.* (2009) Association of genetic variants with myocardial infarction in individuals with or without hypertension or diabetes mellitus. *Int. J. Mol. Med.* **24**, 701–709
8. Pearson, G., Chai, B., Vozheiko, T., Liu, X., Kandarpa, M., Piper, R. C., *et al.* (2018) Clec16a, Nrdp1, and USP8 form a ubiquitin-dependent tripartite complex that regulates beta-cell mitophagy. *Diabetes* **67**, 265–277
9. Jin, S. M., and Youle, R. J. (2012) PINK1- and Parkin-mediated mitophagy at a glance. *J. Cell Sci.* **125**, 795–799
10. Pearson, G., and Soleimanpour, S. A. (2018) A ubiquitin-dependent mitophagy complex maintains mitochondrial function and insulin secretion in beta cells. *Autophagy* **14**, 1160–1161
11. Hain, H. S., Pandey, R., Bakay, M., Strenkowski, B. P., Harrington, D., Romer, M., *et al.* (2021) Inducible knockout of Clec16a in mice results in sensory neurodegeneration. *Sci. Rep.* **11**, 9319
12. Pandey, R., Bakay, M., Hain, H. S., Strenkowski, B., Yermakova, A., Kushner, J. A., *et al.* (2019) The autoimmune disorder susceptibility gene CLEC16A restrains NK cell function in YTS NK cell line and Clec16a knockout mice. *Front. Immunol.* **10**, 68
13. Pandey, R., Bakay, M., Hain, H. S., Strenkowski, B., Elsaqa, B. Z. B., Roizen, J. D., *et al.* (2018) CLEC16A regulates splenocyte and NK cell function in part through MEK signaling. *PLoS One* **13**, e0203952
14. Gingerich, M. A., Liu, X., Chai, B., Pearson, G. L., Vincent, M. P., Stromer, T., *et al.* (2022) An intrinsically disordered protein region encoded by the human disease gene CLEC16A regulates mitophagy. *Autophagy* **19**, 525–543
15. Cheng, Y., LeGall, T., Oldfield, C. J., Dunker, A. K., and Uversky, V. N. (2006) Abundance of intrinsic disorder in protein associated with cardiovascular disease. *Biochemistry* **45**, 10448–10460
16. Du, Z., and Uversky, V. N. (2017) A comprehensive survey of the roles of highly disordered proteins in type 2 diabetes. *Int. J. Mol. Sci.* **18**, 2010
17. Kulkarni, P., and Uversky, V. N. (2019) Intrinsically disordered proteins in chronic diseases. *Biomolecules* **9**, 147
18. Hegyi, H., Buday, L., and Tompa, P. (2009) Intrinsic structural disorder confers cellular viability on oncogenic fusion proteins. *PLoS Comput. Biol.* **5**, e1000552
19. Mei, Y., Glover, K., Su, M., and Sinha, S. C. (2016) Conformational flexibility of BECN1: essential to its key role in autophagy and beyond. *Protein Sci.* **25**, 1767–1785
20. Guharoy, M., Bhowmick, P., and Tompa, P. (2016) Design principles involving protein disorder facilitate specific substrate selection and degradation by the ubiquitin-proteasome system. *J. Biol. Chem.* **291**, 6723–6731
21. Bhowmick, P., Pancsa, R., Guharoy, M., and Tompa, P. (2013) Functional diversity and structural disorder in the human ubiquitination pathway. *PLoS One* **8**, e65443
22. Tunyasuvunakool, K., Adler, J., Wu, Z., Green, T., Zielinski, M., Žídek, A., *et al.* (2021) Highly accurate protein structure prediction for the human proteome. *Nature* **596**, 590–596
23. Varadi, M., Anyango, S., Deshpande, M., Nair, S., Natassia, C., Yordanova, G., *et al.* (2022) AlphaFold protein structure database: Massively

expanding the structural coverage of protein-sequence space with high-accuracy models. *Nucl. Acids Res.* **50**, D439–d444
24. Erdős, G., and Dosztányi, Z. (2020) Analyzing protein disorder with IUPred2A. *Curr. Protoc. Bioinform.* **70**, e99
25. Hatos, A., Hajdu-Soltész, B., Monzon, A. M., Palopoli, N., Álvarez, L., Aykac-Fas, B., *et al.* (2020) DisProt: intrinsic protein disorder annotation in 2020. *Nucl. Acids Res.* **48**, D269–d276
26. Tompa, P. (2002) Intrinsically unstructured proteins. *Trends Biochem. Sci.* **27**, 527–533
27. Uversky, V. N. (2013) The alphabet of intrinsic disorder: II. Various roles of glutamic acid in ordered and intrinsically disordered proteins. *Intrinsic. Disord. Proteins* **1**, e24684
28. Darling, A. L., and Uversky, V. N. (2018) Intrinsic disorder and post-translational modifications: the darker side of the biological dark matter. *Front. Genet.* **9**, 158
29. Fishbain, S., Inobe, T., Israeli, E., Chavali, S., Yu, H., Kago, G., *et al.* (2015) Sequence composition of disordered regions fine-tunes protein half-life. *Nat. Struct. Mol. Biol.* **22**, 214–221
30. van der Lee, R., Lang, B., Kruse, K., Gsponer, J., Sánchez de Groot, N., Huynen, M. A., *et al.* (2014) Intrinsically disordered segments affect protein half-life in the cell and during evolution. *Cell Rep.* **8**, 1832–1844
31. Keul, N. D., Oruganty, K., Schaper Bergman, E. T., Beattie, N. R., McDonald, W. E., Kadirvelraj, R., *et al.* (2018) The entropic force generated by intrinsically disordered segments tunes protein function. *Nature* **563**, 584–588
32. Das, R. K., Ruff, K. M., and Pappu, R. V. (2015) Relating sequence encoded information to form and function of intrinsically disordered proteins. *Curr. Opin. Struct. Biol.* **32**, 102–112
33. Sigrist, C. J., Cerutti, L., Hulo, N., Gattiker, A., Falquet, L., Pagni, M., *et al.* (2002) Prosite: a documented database using patterns and profiles as motif descriptors. *Brief Bioinform.* **3**, 265–274
34. Letunic, I., Khedkar, S., and Bork, P. (2021) Smart: recent updates, new developments and status in 2020. *Nucl. Acids Res.* **49**, D458–d460
35. de Bie, P., and Ciechanover, A. (2011) Ubiquitination of E3 ligases: self-regulation of the ubiquitin system *via* proteolytic and non-proteolytic mechanisms. *Cell Death Differ.* **18**, 1393–1402
36. Radivojac, P., Vacic, V., Haynes, C., Cocklin, R. R., Mohan, A., Heyen, J. W., *et al.* (2010) Identification, analysis, and prediction of protein ubiquitination sites. *Proteins* **78**, 365–380
37. Guharoy, M., Bhowmick, P., Sallam, M., and Tompa, P. (2016) Tripartite degrons confer diversity and specificity on regulated protein degradation in the ubiquitin-proteasome system. *Nat. Commun.* **7**, 10239
38. Jevtić, P., Haakonsen, D. L., and Rapé, M. (2021) An E3 ligase guide to the galaxy of small-molecule-induced protein degradation. *Cell Chem. Biol.* **28**, 1000–1013
39. De Ceuninck, L., Wauman, J., Masschaele, D., Peelman, F., and Tavernier, J. (2013) Reciprocal cross-regulation between RNF41 and USP8 controls cytokine receptor sorting and processing. *J. Cell Sci.* **126**, 3770–3781
40. Wu, X., Yen, L., Irwin, L., Sweeney, C., and Carraway, K. L., 3rd. (2004) Stabilization of the E3 ubiquitin ligase Nrdp1 by the deubiquitinating enzyme USP8. *Mol. Cell Biol.* **24**, 7748–7757
41. Qiu, X. B., and Goldberg, A. L. (2002) Nrdp1/FLRF is a ubiquitin ligase promoting ubiquitination and degradation of the epidermal growth factor receptor family member, ErbB3. *Proc. Natl. Acad. Sci. U. S. A.* **99**, 14843–14848
42. Babu, M. M. (2016) The contribution of intrinsically disordered regions to protein function, cellular complexity, and human disease. *Biochem. Soc. Trans.* **44**, 1185–1200
43. Popelka, H., Uversky, V. N., and Klionsky, D. J. (2014) Identification of Atg3 as an intrinsically disordered polypeptide yields insights into the molecular dynamics of autophagy-related proteins in yeast. *Autophagy* **10**, 1093–1104
44. Sahu, D., Bastidas, M., and Showalter, S. A. (2014) Generating NMR chemical shift assignments of intrinsically disordered proteins using carbon-detected NMR methods. *Anal. Biochem.* **449**, 17–25
45. Kelly, S. M., Jess, T. J., and Price, N. C. (2005) How to study proteins by circular dichroism. *Biochim. Biophys. Acta* **1751**, 119–139
46. Uversky, V. N. (2009) Intrinsically disordered proteins and their environment: effects of strong denaturants, temperature, pH, counter ions, membranes, binding partners, osmolytes, and macromolecular crowding. *Protein J.* **28**, 305–325
47. Durcan, T. M., Tang, M. Y., Perusse, J. R., Dashti, E. A., Aguileta, M. A., McLelland, G. L., *et al.* (2014) USP8 regulates mitophagy by removing K6-linked ubiquitin conjugates from parkin. *EMBO J.* **33**, 2473–2491
48. Pearson, G. L., Gingerich, M. A., Walker, E. M., Biden, T. J., and Soleimanpour, S. A. (2021) A selective look at autophagy in pancreatic β-cells. *Diabetes* **70**, 1229–1241
49. Zhong, L., Tan, Y., Zhou, A., Yu, Q., and Zhou, J. (2005) RING finger ubiquitin-protein isopeptide ligase Nrdp1/FLRF regulates parkin stability and activity. *J. Biol. Chem.* **280**, 9425–9430
50. Hagai, T., Azia, A., Tóth-Petróczy, Á., and Levy, Y. (2011) Intrinsic disorder in ubiquitination substrates. *J. Mol. Biol.* **412**, 319–324
51. Yang, J., Gao, M., Xiong, J., Su, Z., and Huang, Y. (2019) Features of molecular recognition of intrinsically disordered proteins *via* coupled folding and binding. *Protein Sci.* **28**, 1952–1965
52. Davey, N. E., Seo, M. H., Yadav, V. K., Jeon, J., Nim, S., Krystkowiak, I., *et al.* (2017) Discovery of short linear motif-mediated interactions through phage display of intrinsically disordered regions of the human proteome. *FEBS J.* **284**, 485–498
53. Das, R. K., Mao, A. H., and Pappu, R. V. (2012) Unmasking functional motifs within disordered regions of proteins. *Sci. Signal.* **5**, pe17
54. Ali, M., Simonetti, L., and Ivarsson, Y. (2020) Screening intrinsically disordered regions for short linear binding motifs. *Met. Mol. Biol.* **2141**, 529–552
55. Lieutaud, P., Ferron, F., Uversky, A. V., Kurgan, L., Uversky, V. N., and Longhi, S. (2016) How disordered is my protein and what is its disorder for? A guide through the "dark side" of the protein universe. *Intrinsic. Disord. Proteins* **4**, e1259708
56. Theillet, F. X., Binolfi, A., Frembgen-Kesner, T., Hingorani, K., Sarkar, M., Kyne, C., *et al.* (2014) Physicochemical properties of cells and their effects on intrinsically disordered proteins (IDPs). *Chem. Rev.* **114**, 6661–6714
57. Mero, I. L., Ban, M., Lorentzen, A. R., Smestad, C., Celius, E. G., Saether, H., *et al.* (2011) Exploring the CLEC16A gene reveals a MS-associated variant with correlation to the relative expression of CLEC16A isoforms in thymus. *Genes Immun.* **12**, 191–198
58. Claiborn, K. C., Sachdeva, M. M., Cannon, C. E., Groff, D. N., Singer, J. D., and Stoffers, D. A. (2010) Pcif1 modulates Pdx1 protein stability and pancreatic β cell function and survival in mice. *J. Clin. Invest.* **120**, 3713–3721
59. Stothard, P. (2000) The sequence manipulation suite: JavaScript programs for analyzing and formatting protein and DNA sequences. *Biotechniques* **28**, 1104
60. Diamonti, A. J., Guy, P. M., Ivanof, C., Wong, K., Sweeney, C., and Carraway, K. L., 3rd (2002) An RBCC protein implicated in maintenance of steady-state neuregulin receptor levels. *Proc. Natl. Acad. Sci. U. S. A.* **99**, 2866–2871
61. Wauman, J., De Ceuninck, L., Vanderroost, N., Lievens, S., and Tavernier, J. (2011) RNF41 (Nrdp1) controls type 1 cytokine receptor degradation and ectodomain shedding. *J. Cell Sci.* **124**, 921–932
62. Cunningham, F., Allen, J. E., Allen, J., Alvarez-Jarreta, J., Amode, M. R., Armean, I. M., *et al.* (2022) Ensembl 2022. *Nucl. Acids Res.* **50**, D988–d995
63. Madeira, F., Pearce, M., Tivey, A. R. N., Basutkar, P., Lee, J., Edbali, O., *et al.* (2022) Search and sequence analysis tools services from EMBL-EBI in 2022. *Nucl. Acids Res.* **50**, W276–279
64. Larkin, M. A., Blackshields, G., Brown, N. P., Chenna, R., McGettigan, P. A., McWilliam, H., *et al.* (2007) Clustal W and clustal X version 2.0. *Bioinformatics* **23**, 2947–2948
65. Ashkenazy, H., Abadi, S., Martz, E., Chay, O., Mayrose, I., Pupko, T., *et al.* (2016) ConSurf 2016: an improved methodology to estimate and visualize evolutionary conservation in macromolecules. *Nucl. Acids Res.* **44**, W344–350